Journal of the Meteorological Society of Japan, Vol. 89, No. 4, pp. 327–340, 2011
DOI:10.2151/jmsj.2011-403

Effects of Solar Radiation Amount and Synoptic-scale Wind on the Local Wind "Karakkaze" over the Kanto Plain in Japan

Hiroyuki KUSAKA

Center for Computational Sciences, University of Tsukuba, Tsukuba, Japan

Yukako MIYA and Ryosaku IKEDA

Graduate School of Life and Environmental Sciences, University of Tsukuba, Tsukuba, Japan

(Manuscript received 21 August 2009, in final form 30 May 2011)

Abstract

A climatological and numerical study of "Karakkaze," a type of local wind in Japan, was conducted. First, winter days under a winter-type synoptic pressure pattern with daily minimum relative humidity of less than 40% were classified according to strong wind (wind speed $\geqq 9$ ms^{-1}, Karakkaze day), medium wind (6 ms^{-1} $\leqq$ wind speed < 9 ms^{-1}), and weak wind (wind speed < 6 ms^{-1}). Secondly, the spatial patterns of the surface wind in each category are confirmed by the Japan Meteorological Agency (JMA)-Automated Meteorological Data Acquisition System (AMeDAS) observation data. In addition, we compared the boundary-layer wind of the three categories using wind speed data from the observation tower of the Meteorological Research Institute (MRI) in Tsukuba and from the JMA wind profiler in Kumagaya. Finally, we performed one-dimensional numerical experiments using a column Planetary Boundary Layer (PBL) model to evaluate the impact of solar radiation and upper-level wind on the formation of the Karakkaze.

The results are summarized as follows. On the strong-wind days, strong northwesterly winds appear in the area along the Arakawa River and the Tonegawa River from Maebashi. The surface wind speed has a clear diurnal variation with a peak in the early afternoon. Such a diurnal variation is observed up to a 200 m level, but this diurnal pattern nearly reverses itself between 200 m and 400 m levels. On weak-wind days, the diurnal variation pattern is similar to that in other two categories, but the reversed pattern appears at a 100 m level, not at a 200 m level.

Stronger surface winds appear under a clearer winter-type pressure pattern. The correlation coefficient is 0.632 between the daily maximum surface wind speed and the daily mean wind speed at a height of 2759 m, whereas the correlation is 0.284 between the surface wind speed and daily sunshine duration, which, in a previous study, was suggested to be the most significant factor.

Numerical experiments indicate that a large amount of solar radiation is a necessary condition for a strong daytime wind, but this is not a sufficient explanation for the difference in the surface wind speed between weak and strong-wind days.

1. Introduction

Japan is mountainous (Fig. 1), and thus produces a variety of thermally and dynamically driven local winds (Arakawa 1971, Yoshino 1986) such as the "Yamaji-Kaze" (Furukawa 1966, Saito and Ikawa 1991, Saito 1994), "Hirodo-Kaze" (Nakamura et al. 2002, Fudeyasu et al. 2008), "Kiyokawa-Dashi" (Takeuchi 1986, Yamagishi and Kato 1996, Ishii et al. 2007, Sasaki et al. 2010), and "Karakkaze" (Yoshino 1986, Yomogida and Rikiishi 2004, Miya and Kusaka 2009). The Karakkaze is a dry, strong, northwesterly local wind on the Kanto Plain under a typical winter-type pressure pat-

Corresponding author: Hiroyuki Kusaka, Center for Computational Sciences, University of Tsukuba, Tsukuba, Ibaraki 305-8577, Japan.
E-mail: kusaka@ccs.tsukuba.ac.jp

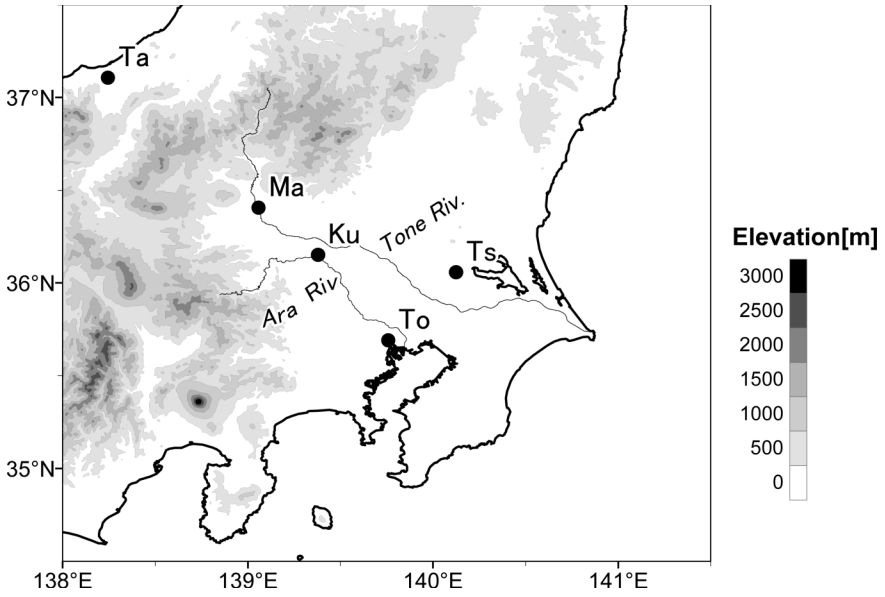

Fig. 1. Topography of Central Japan. The solid circle indicates meteorological observation stations. Ta is Takada; Ma, Maebashi; Ku, Kumagaya; Ts, Tsukuba; and To, Tokyo. Ara Riv is the Arakawa River and Tone Riv is the Tonegawa River.

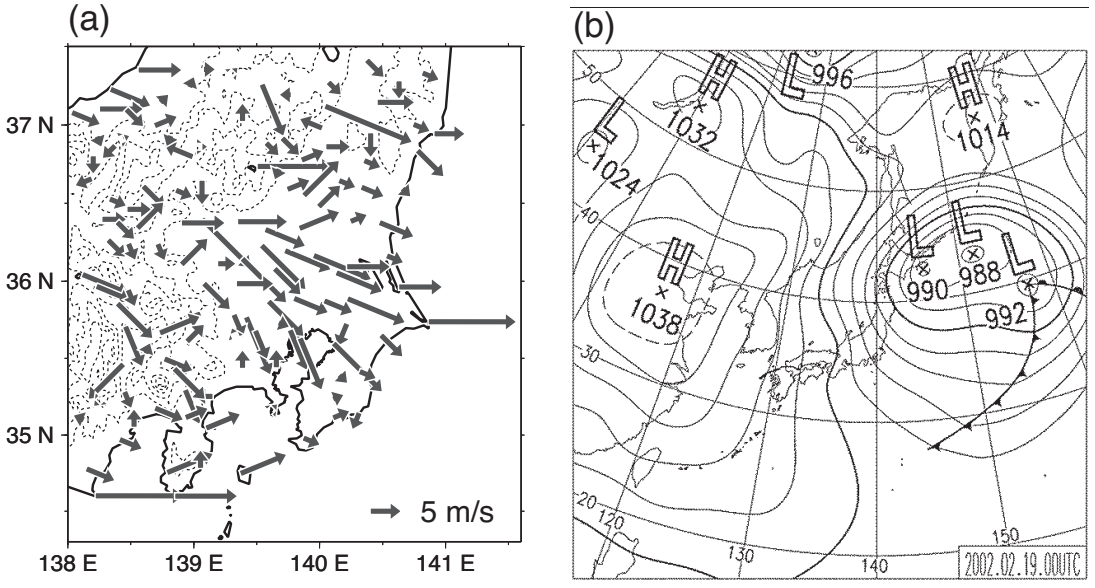

Fig. 2. A typical case of the Karakkaze. (a) Surface wind at 1400 JST 19 February 2002 and (b) surface weather chart at 0900 JST 19 February 2002.

tern (Yoshino 1986) (Fig. 2).

Kawamura (1966) analyzed several airstream patterns in central Japan in winter that suggested that the Karakkaze is a typical winter flow pattern on the Kanto Plain. Yoshino (1970) shows the horizontal distribution of the wind, temperature, and relative humidity on a winter day when strong northwesterly winds occur on the Kanto Plain; in addition, in this paper, we illustrate

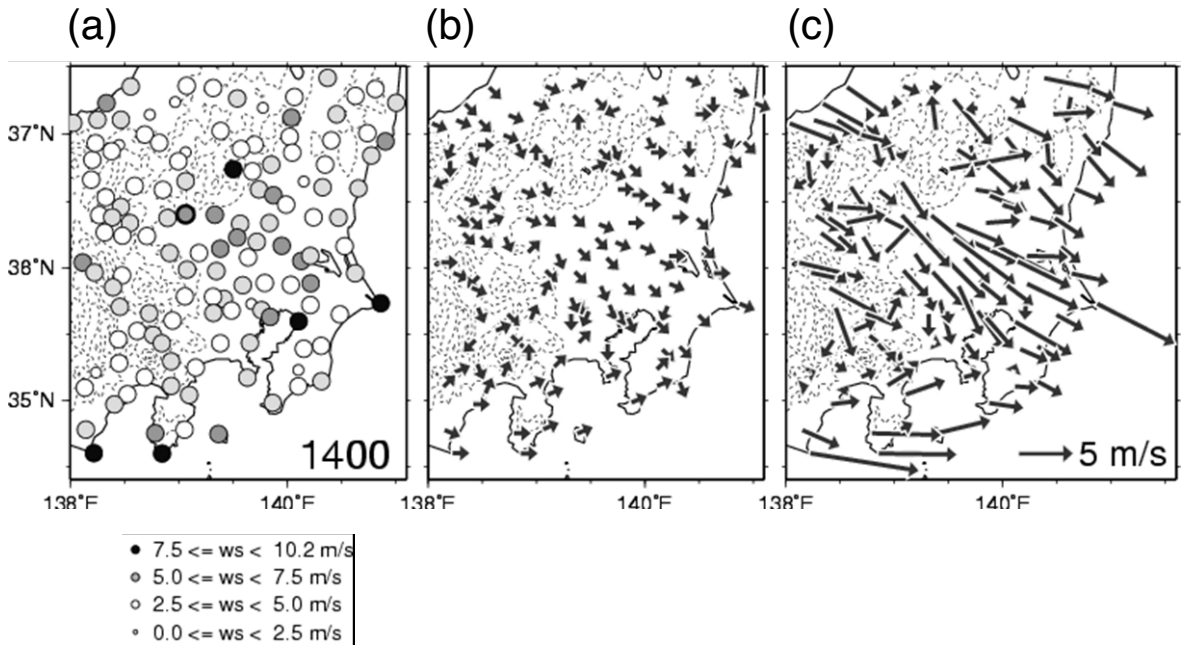

Fig. 3. (a) Mean wind speed at 1400 JST,(b) most frequent wind direction, and (c) wind vector averaged at 1400 JST of the 135 strong wind day average. The circle with thick solid line indicates the value at the Maebashi observation site (36.405N, 139.006E).

the vertical cross sections of the wind speed and relative humidity from the Sea of Japan (upward area) to the Pacific Ocean (leeward area) by way of the mountains. Yoshino (1970) reported that the Karakkaze with large wind speed is a Bora-type downslope wind. On the other hand, Yamagishi (2002) and Yomogida and Rikiishi (2004) reported that *the strong Karakkaze is caused by an efficient momentum transfer from aloft through the evolving convective boundary layer*. In addition, they described a strong wind as *one mainly formed and maintained by strong solar radiation*. Their idea is that the speed of Karakkaze has a clear diurnal variation with a maximum value in the early afternoon and wind speeds increase as the duration of sunshine is longer. Miya and Kusaka (2009) examined the vertical structure of the Karakkaze and compared it to the winter average. They described the Karakkaze as being formed by the downward momentum transfer from the ambient wind. However, their conclusions are preliminary and have not been quantitatively analyzed. Therefore, current information regarding the Karakkaze is limited.

The present study is a statistical and numerical investigation of the effects of the amount of solar radiation and synoptic-scale wind speed on the Karakkaze.

2. Data and Methodology

In this study, a Karakkaze is defined as wind under a winter-type synoptic pressure pattern with daily minimum relative humidity of less than 40% and daily maximum wind speed of more than 9 m s^{-1} (with reference to Miya and Kusaka 2009). A Karakkaze day is one when a wind meeting the above conditions is observed at Maebashi station. Maebashi station was chosen since the Karakkaze is known to be the most pronounced in the vicinity of the station (Yoshino 1986).

Hereafter, a Karakkaze day is referred to as a strong-wind day in the present study. Similar to the definition of a strong-wind day, two more wind classifications used in the present study on the basis of the daily maximum wind speed at Maebashi station are a medium-wind day (*wind speed of more than or equal to 6 m* s^{-1} *and less than 9 m* s^{-1}) and a weak-wind day (*wind speed of less than 6 m* s^{-1}). All parameters except the wind speed are kept as constants among the strong, medium, and weak-wind days.

We investigate the variability of the daily maximum wind speed in determining the characteristics of the spatial distribution and the formation mechanisms of the Karakkaze. A statistical analysis is performed for

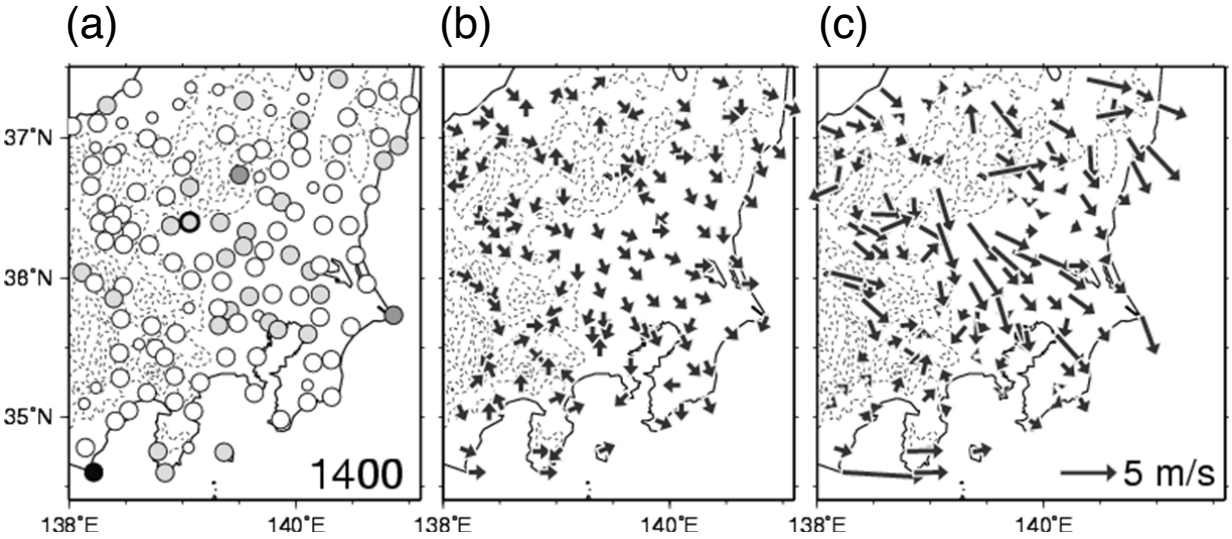

Fig. 4. Same as Fig. 4, but for the 379 medium wind day average.

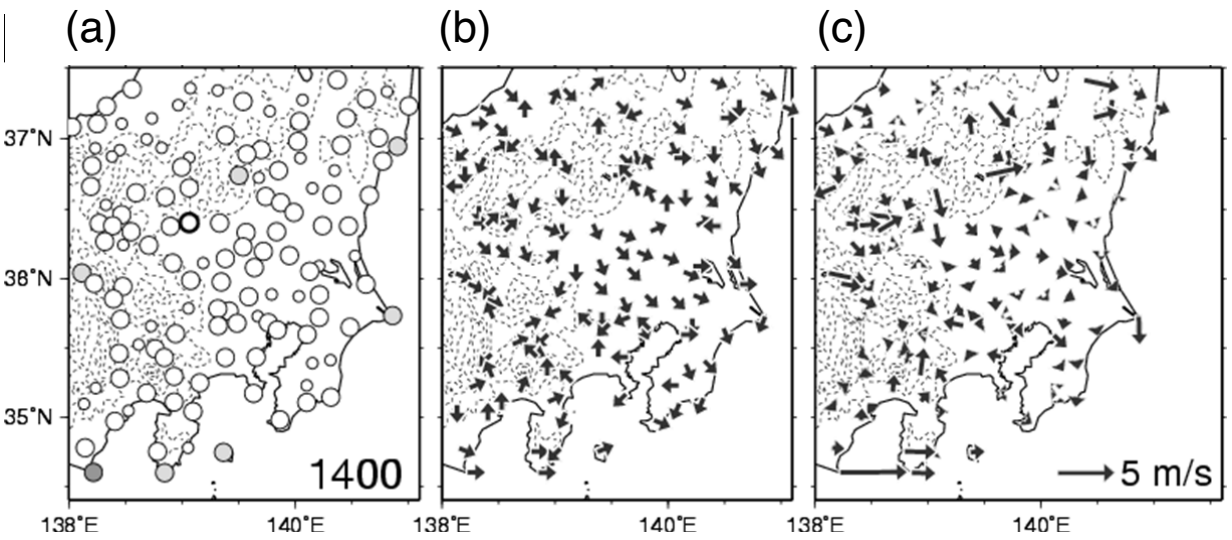

Fig. 5. Same as Fig. 3, but for the 159 weak wind day average.

the winter seasons (December through February) from 1992 to 2006. Observational data used in the present study are station data obtained by the Japan Meteorological Agency (JMA); surface observation data from the Automated Meteorological Data Acquisition System (AMeDAS) network in the Kanto area and Takada, Maebashi, Kumagaya, Tsukuba, and Tokyo meteorological observatories for 1992–2005; radio sonde data from Tsukuba aerological observatories for 1998–2005; tower data from Meteorological Research Institute (MRI) at Tsukuba for 1992–1999; wind profiler data from the Wind profiler Network and Data Acquisition System (WINDAS) at Takada and Kumagaya for December 2002–2005; and Japanese 25-year Re-Analysis (JRA-25, Onogi et al. 2007) and JMA Climate Assimilation Data System (JCDAS) global analysis data for 1992–2006.

3. Statistical Analysis

3.1 Surface wind systems

A comparison of the daytime surface wind system among strong, medium, and weak-wind days is presented in Figures 3–5. On strong-wind days, northwesterly winds of over 5 m s^{-1} appear in coastal areas and the area between the Arakawa River and the Tonegawa River (Fig. 3). However, the wind is weak on most of the plain except for the inland areas around Maebashi, Kumagaya and in the vicinity of some coastal stations on medium-wind days (Fig. 4). On weak-wind days, surface winds are weak over the entire Kanto Plain and the wind direction is not spatially homogeneous (Fig. 5). Areas with a strong surface wind speed expand south and southeastward as the wind speed at Maebashi becomes stronger.

3.2 Diurnal variation of the wind speed in the boundary layer

Figure 6a shows the diurnal variation of the wind speed, which is the average of the strong-wind days observed from the 213 m tower of the Meteorological Research Institute (MRI) at Tsukuba. On strong-wind days, the wind speed near the surface shows a clear diurnal variation; the daytime wind speed is strong but weakens at night. The diurnal pattern is similar at all levels with the exception of a late start time of the increase in the wind speed and a temporal wind speed reduction above 100 m just after sunrise (Fig. 6a). On medium-wind days, the diurnal pattern is similar to that on strong-wind days (Fig. 6b).

However, on weak-wind days, the diurnal pattern is very different from those of the strong and medium-wind days (Fig. 6c). The wind speed at 10 m has a clear diurnal variation with a peak at around noon, which is one or two hours earlier than that of the medium and strong-wind days. The diurnal variation at 25 m is similar to that of the 10 m level, but there are some significant differences. The amplitude is smaller, the wind speed temporarily decreases just after sunrise, and the wind speed does not largely decrease in the afternoon. At the 50, 100, and 200 m levels, the wind speed decreases sharply following sunrise, attains a small value around noon, and increases in the early evening. Such a feature indicates the decoupled phenomena occurring around 100 m at night on weak-wind days. Indeed, the nocturnal atmospheric stability near the surface is very strong on weak-wind days; the strength of the surface inversion between 10 m and 100 m levels is -1.0, -2.0, and -3.5 K on strong, medium, and weak-wind days, respectively (fig. is omitted).

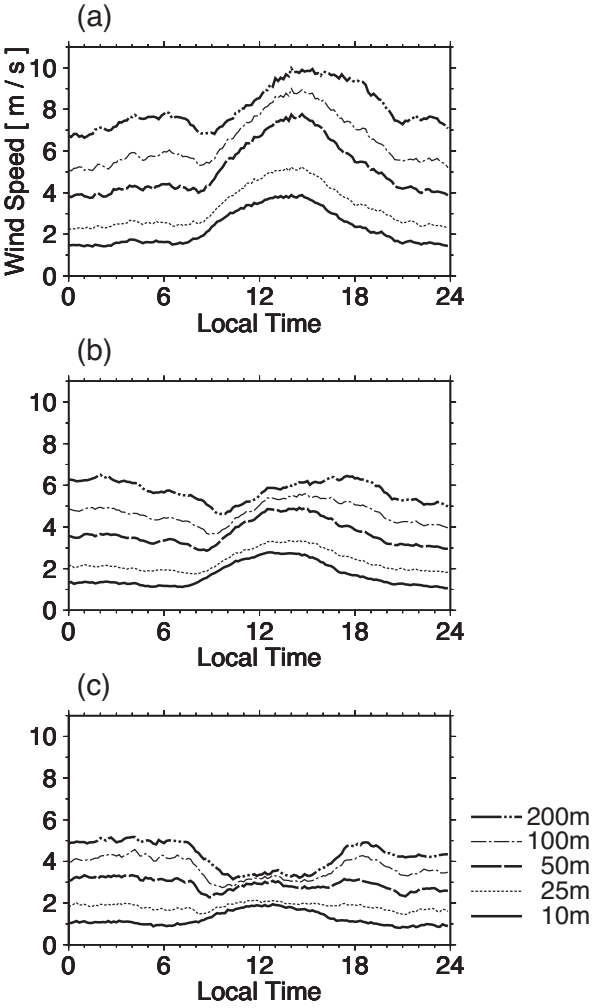

Fig. 6. Diurnal variation of wind speed from the MRI tower at Tsukuba. (a) Average of 74 strong wind days, (b) average of 194 medium wind days, and (c) average of 75 weak wind days. The lines indicate the observation height above ground level.

The diurnal variation of the wind speed observed from the wind profiler and the surface meteorological observation station at Kumagaya is shown in Fig. 7. Here, the wind speed is the average of the strong, medium, and weak-wind days. On strong-wind days, the diurnal pattern at 394 m is different from those of the weak and medium-wind days (Fig. 7a). It is similar to that at 200 m on medium-wind days. The diurnal pattern of wind speed at 394 m on medium-wind days is similar to that at the 200 m and 100 m levels on weak-

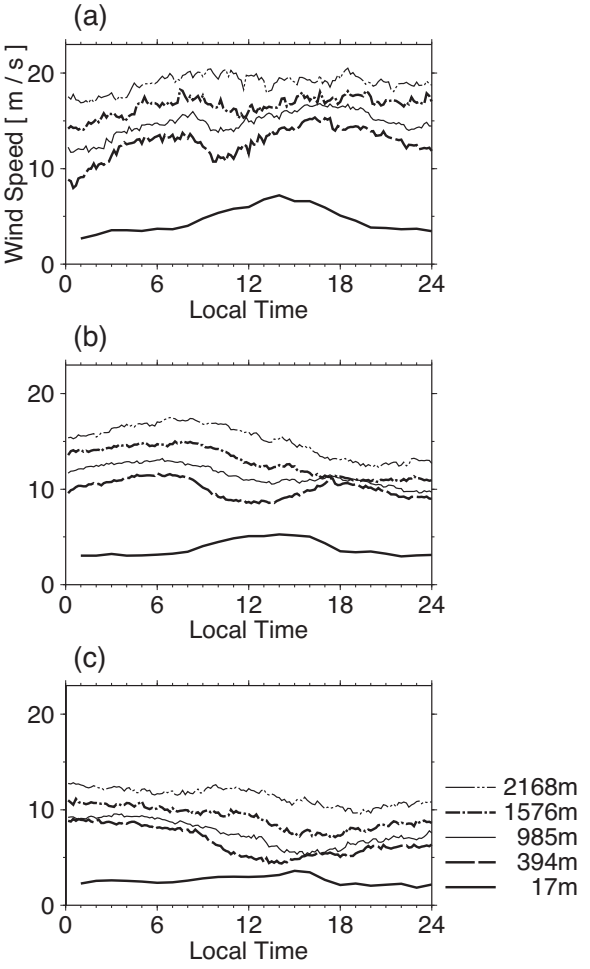

Fig. 7. Diurnal variation of wind speed from the wind profiler at Kumagaya. (a) Average of 36 strong wind days, (b) average of 113 medium wind days, and (c) average of 55 weak wind days. The lines indicate the height above ground level.

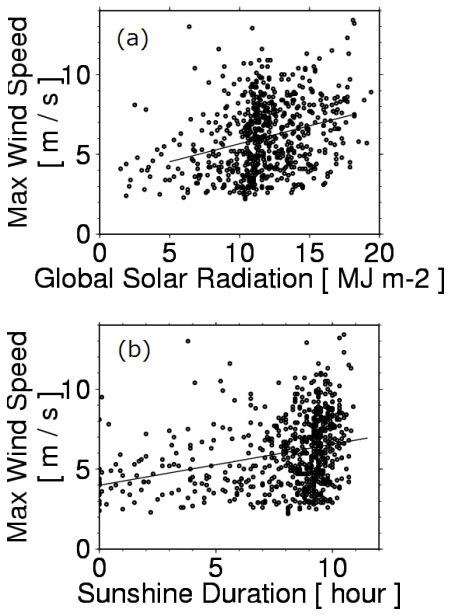

Fig. 8. (a) Relationship between the daily maximum surface wind speed and daily global solar radiation amount at Tsukuba on strong, medium, and weak wind days. (b) Relationship between the daily maximum surface wind speed and daily sunshine duration time at Tsukuba on strong, medium, and weak wind days.

wind days (Fig. 7b). On weak-wind days, the diurnal variation pattern at 394 m is similar to that at the 200 m and 100 m levels (Fig. 7c).

Results of the analysis from the tower and wind profiler data indicate that the height at which a wind system with the same diurnal variation pattern as the surface wind is observed increases as the Karakkaze increases in strength (Figs. 6, 7). In other words, the surface affects the wind at the higher levels as the Karakkaze becomes stronger. Another important fact is that the wind speed at 1,576 m, which is in the free atmosphere, is larger when the Karakkaze is stronger. In addition, the daytime wind shear is larger between the 17 m and 394 m levels.

At the MRI tower, a seasonal dependence is evident in the heights at which the reversal of the diurnal variation is observed. The heights of the reversals are at 100 m or less in winter and 200 m or more in summer (Fujitani 1985). Since the boundary layer is more thoroughly mixed in the summer than in the winter, the higher reversal level means a more thoroughly mixed lower boundary layer. We can infer that strong-wind days, rather than weak-wind days, coincide with a well-mixed lower boundary layer.

These results suggest that the momentum descends to the ground with sunrise on the Karakkaze days and a larger momentum descends to the ground more effectively on stronger-wind days.

3.3 Relationship between the surface wind speed and environmental conditions

In this section, we investigate potential factors affecting the strength of the well-mixed lower boundary

Table 1. Daily precipitation amount, daily minimum relative humidity, and daily global solar radiation amount. Average of 159 weak wind days, average of 379 medium wind days, and average of 135 strong wind days.

Station	Daily precipitation amount [mm]			Daily minimum relative humidity [%]			Daily global solar radiation amount [M J m^{-2}]		
	Weak	Medium	Strong	Weak	Medium	Strong	Weak	Medium	Strong
Takada	16.0	19.5	18.3	60.3	60.1	53.2	6.1	4.6	4.8
Maebashi	0.0	0.1	0.6	29.2	29.0	25.7	11.0	11.3	12.0
Kumagaya	0.0	0.1	0.7	27.8	26.6	23.3	—	—	—
Tsukuba	0.1	0.3	1.0	32.0	29.3	25.3	11.3	11.8	12.3
Tokyo	0.2	0.3	1.0	27.9	25.3	20.6	10.3	10.9	11.6

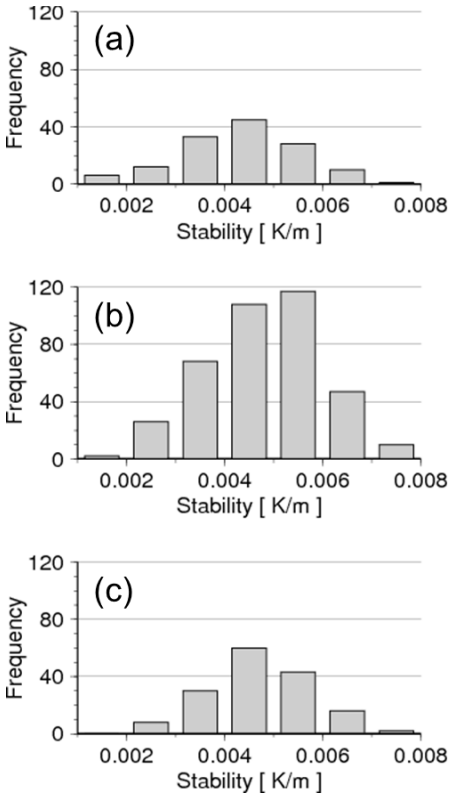

Fig. 9. Frequency of occurrence of potential temperature lapse rates at Tateno sonde station for (a) strong, (b) medium, and (c) weak wind days.

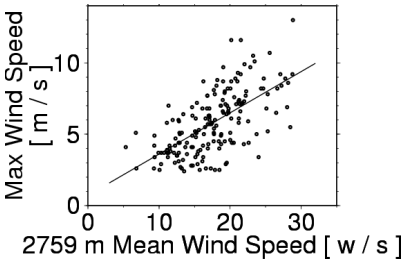

Fig. 10. Relationship between the daily maximum surface wind speed at Tsukuba and daily mean wind speed at 2759 m level from the wind profiler at Kumagaya on strong, medium, and weak wind days.

layer on strong-wind days. The relationship between the daily maximum speed of the surface wind and the amount of daily global solar radiation at Tsukuba is investigated statistically. A scatter diagram to confirm the contribution of the buoyancy to convection at Tsukuba is shown in Fig. 8a. The correlation coefficient is 0.304 between the amount of daily solar radiation and the speed of daily maximum surface wind. The amount of daily solar radiation on strong-wind days is 0.5 MJ m^{-2} and 1.0 MJ m^{-2} larger than that of medium and weak-wind days, respectively (Table 1). Such a tendency is seen in Maebashi and Tokyo. The relationship between the daily sunshine duration and daily maximum surface wind speed in Tsukuba is shown in Fig. 8b. The correlation is only 0.284, which is not very high.

The background atmospheric stability also affects the boundary layer height and mixing in the boundary layer. The frequency of occurrence for potential temperature lapse rates for strong, medium, and weak-wind days is shown in Fig. 9. The average lapse rate on strong-wind days is less stable than that on weak-wind days, but the difference is very small. Thus, the impact will be very small in the present cases although a weaker lapse rate produces a higher boundary layer.

Here, we focus on the wind in the outer layer, as the surface wind speed is dependent on the Rossby-number similarity theory under a neutral atmospheric condition. Statistical analysis of wind profiler data shows that the

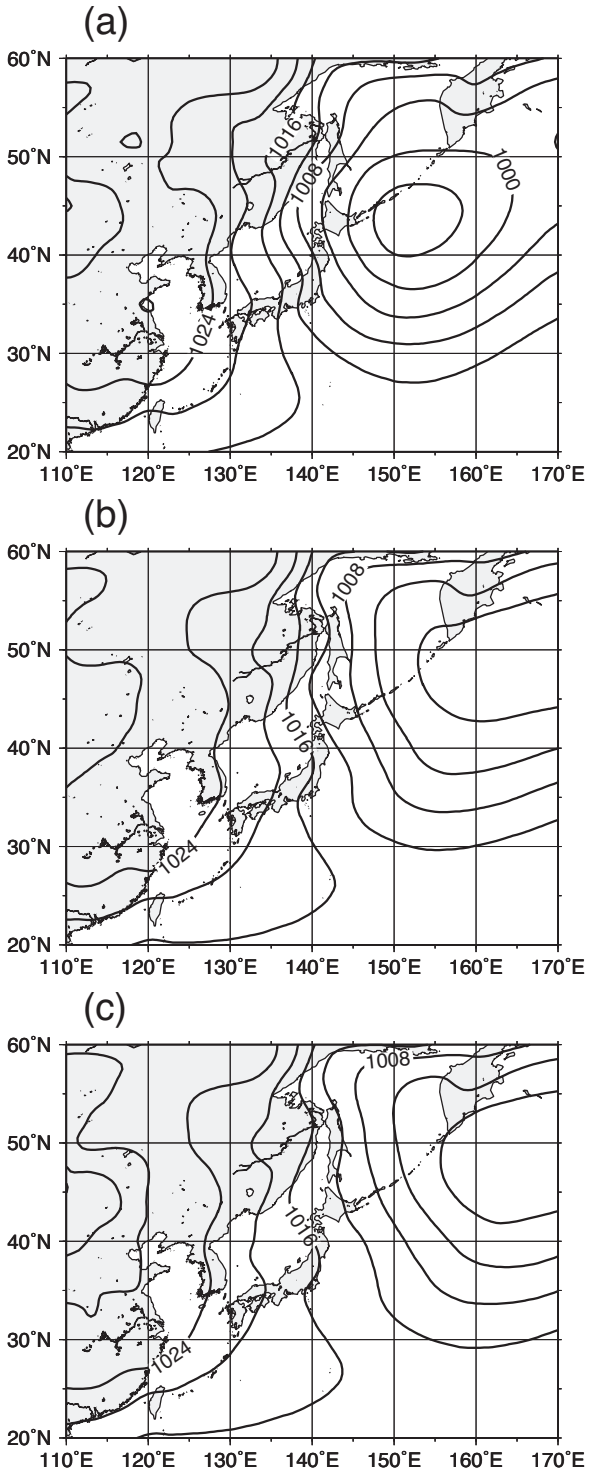

Fig. 11. Composite of sea-level pressure at 1500 JST. (a) 113 strong wind days, (b) 181 medium wind days, and (c) 100 weak wind days.

wind blows more strongly when the upper-level wind is stronger (Fig. 10). The correlation coefficient is 0.632 (confidence interval, 99%).

The sea-level pressure patterns created from the JRA-25 analysis data indicate that the east-west pressure gradient associated with a clear typical winter-type pressure pattern is large when the Karakkaze is strong (Fig. 11). These results suggest that the cold outbreak associated with the winter-type pressure pattern produces a strong, cold, Bora-like wind (e.g., Yoshino 1986) that flows over the Chubu mountains and reaches the leeward Kanto Plain. As a result, the wind mainly leads to a clear sky on the plain and transportation of large momentum to the ground.

4. Numerical Experiments

4.1 Description of the numerical model and design of numerical experiments

Numerical experiments using a simple one-dimensional PBL model are conducted to confirm the sensitivity of the surface wind speed to the synoptic-scale wind and amount of solar radiation. Simulations using such a simple model provide us with the comprehensible results that are necessary to examine the "potential impact" of the above two factors, although they also have disadvantages such as the omission of mountainous terrain.

The PBL model used in the present study is a one-dimensional column model, which is a one-dimensional version of the LCM2D used in Kusaka and Kimura (2004a, b). The governing equations of the model are

$$\frac{\partial u}{\partial t} = f(v - v_g) + \frac{\partial}{\partial z}\left(K_m \frac{\partial u}{\partial z}\right) \quad (1)$$

$$\frac{\partial v}{\partial t} = -f(u - u_g) + \frac{\partial}{\partial z}\left(K_m \frac{\partial v}{\partial z}\right) \quad (2)$$

$$\frac{\partial \theta'}{\partial t} = \frac{\partial}{\partial z}\left(K_h \frac{\partial \theta'}{\partial z}\right) \quad (3)$$

Here, the first term on the right-hand side consists of the Coriolis and environmental pressure gradient terms. u_g and v_g are, respectively, the east-west and north-south components of the geostrophic wind velocity. θ' is the perturbation from the base-state potential temperature, Θ. The base-state potential temperature is 278.4 K. K_m and K_h are the vertical diffusion coefficients for the momentum and heat, respectively. They are estimated using the Mellor-Yamada turbulent closure model level at 2 (Mellor and Yamada 1974). Short and long-wave radiation is calculated following Kondo (1994). A Newtonian cooling scheme is also adopted. Surface fluxes are calculated using the Louis (1979) for-

Table 2. Surface parameters used in the model.

Parameters	Value
Thermal conductivity	1.6 [W m^{-1} K^{-1}]
Heat capacity	2.0 * 10^6 [J m^{-3} K^{-1}]
Roughness length	0.1 [m]
Moisture availability	0.3
Albedo	0.2
Emissivity	0.97

mula. Surface skin temperature is estimated by solving the surface heat budget equation. Soil temperature is calculated by utilizing the thermal diffusion model. The surface parameters used in the scheme are summarized in Table 2. For the time integration, the Euler forward scheme is used to calculate the Coriolis and environmental pressure gradient terms, and the backward scheme is used for diffusion terms. For the spatial difference, the 2nd-order centered scheme is used.

Control experiments are conducted for the weak-wind day (Case 1) and the strong-wind day (Case 2). In addition, sensitivity experiments are performed to confirm the impact of the amount of solar radiation (Case 3), synoptic-scale wind (Case 4), and background atmospheric stability (Case 5) on the surface wind speed (Table 3).

The numerical integration of all experiments was started at 00 Local Solar Time (LST) January 1st. Initial conditions were created from the climatological mean of observations. The initial potential temperature lapse rate was set to 0.0048 K m^{-1} for Cases 1 and 5 and 0.0044 K m^{-1} for Cases 2–4 in accordance with Kusaka et al. (2000); the initial surface potential temperature was 278.4 K; the initial relative humidity was 35%, which is vertically constant for all cases; and a vertically constant geostrophic wind velocity of 12 m s^{-1} was set as an initial wind velocity for Cases 1 and 3 and 19 m s^{-1} for Cases 2, 4, and 5. The Dirichlet boundary condition was set at the model top. The surface boundary condition was given by the surface fluxes. The model was run for 72 hours and the results of the 3rd day after the initial time are examined; the first two days were used as a spin-up to remove the effects of the initial condition in the atmospheric boundary layer.

4.2 Results

The diurnal variation of the wind speed is simulated well in the control case for a weak-wind day (Case 1), including the decoupled phenomenon between the 110.5 m and 30.5 m levels (Fig. 12a). A low-level jet, which is an essential feature of the PBL model (e.g., Blackadar 1957, Yamamoto et al. 1973), is also qualitatively reproduced at the 210.5 m level. In the control case for a strong-wind day (Case 2), the diurnal wind speed at the 110.5 m and 210.5 m levels is not well reproduced (Fig. 12b). However, it is similar to the observation at 394 m. In addition, the low-level jet is also simulated above 300 m (although the line is omitted in the figure). For these reasons, it is considered that the PBL model simulates the difference in the basic feature of the wind between the weak and strong-wind days; the surface wind speed on the strong-wind day is larger than that of the weak-wind day, and the diurnal variation with a daytime peak is higher on a strong-wind day than a weak-wind day.

A sensitivity experiment with a large quantity of solar radiation (Case 3) shows that the difference in the amount of solar radiation between the strong and weak-wind days has only a slight effect on the formation of strong wind near the surface (Figs. 12a, c). Indeed, the amount of enhanced solar radiation increases the momentum diffusion coefficient associated with the enhanced buoyancy (Fig. 13a). However, there is some sensitivity of momentum transfer (Fig. 13b) because of the small wind shear. In addition, the PBL height from Case 3 is comparable to that of Case 1 (Figs. 13a, b). From these results, the difference in the amount of solar radiation is not a sufficient explanation for the strong wind in the afternoon, although the amount of solar radiation is a necessary condition to couple the surface wind with upper-level wind and to increase the surface

Table 3. Configurations of the numerical experiments.

Name of case	Experiment	Wind speed at the top boundary [m s^{-1}]	Global solar radiation amount [MJ m^{-2}]	Lapse rate of potential temperature [K m^{-1}]
1	Control for weak wind day	12	11.4	0.0048
2	Control for strong wind day	19	12.3	0.0044
3	Weak wind speed	12	12.3	0.0044
4	Small radiation amount	19	11.4	0.0044
5	Strong Atmospheric Stability	19	12.3	0.0048

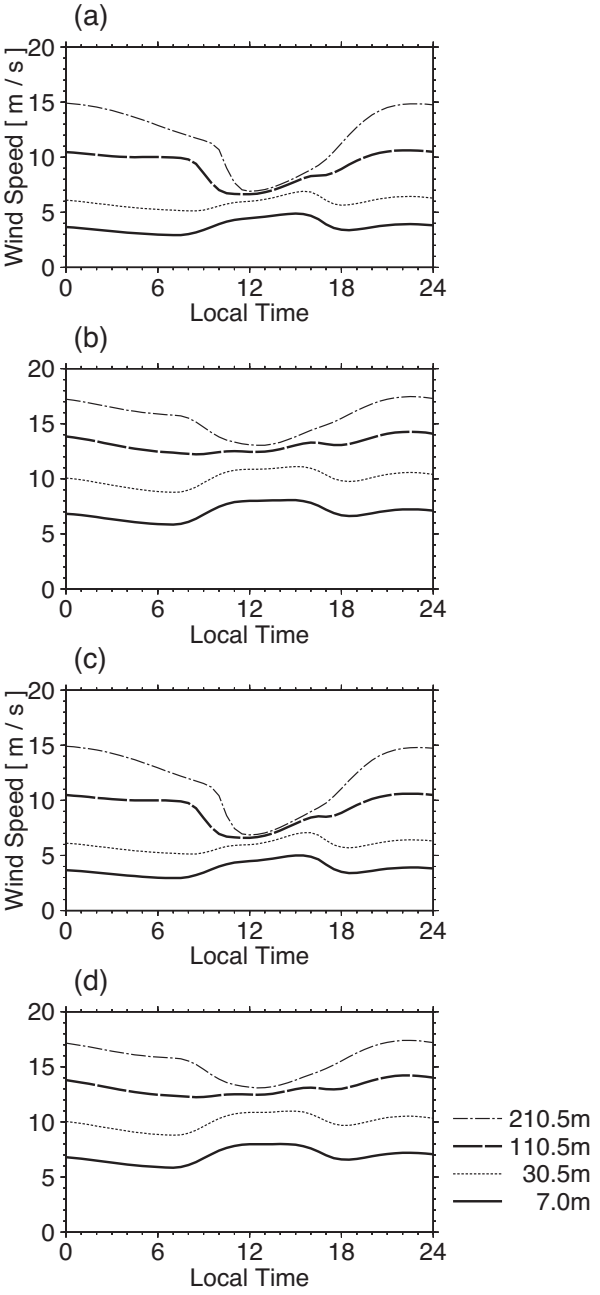

Fig. 12. Diurnal variation of wind speed from the numerical experiments. (a) Case 1, (b) Case 2, (c) Case 3, and (d) Case 4.

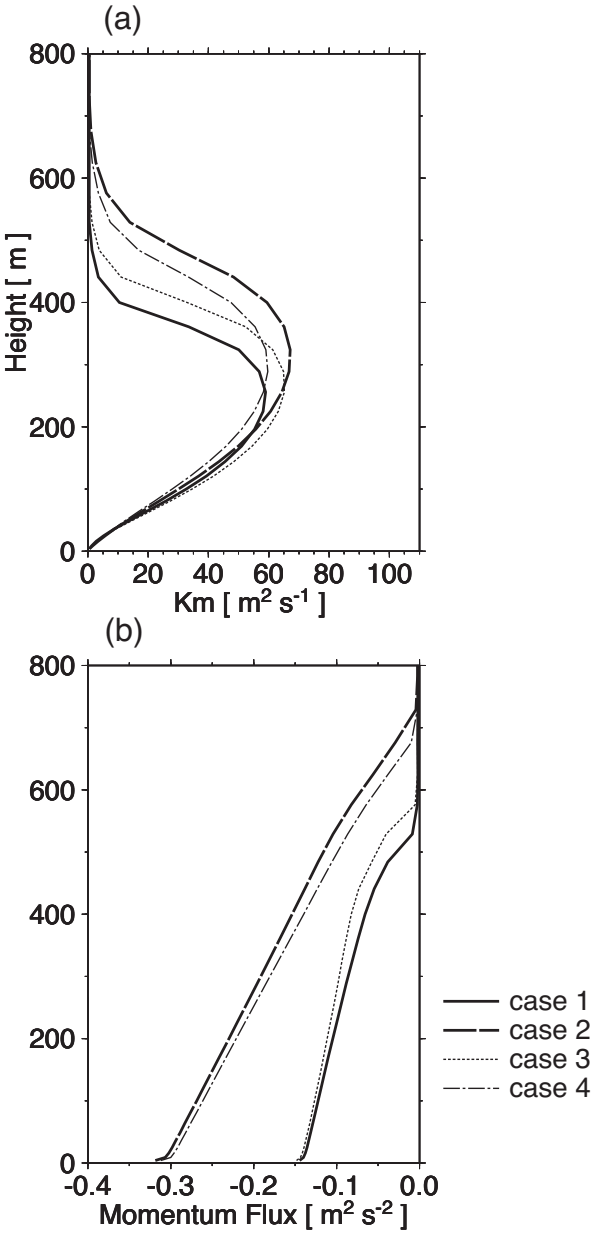

Fig. 13. Vertical profile of (a) diffusion coefficient for momentum and (b) momentum flux at 1400 JST from the numerical experiments.

wind speed in the morning.

On the other hand, a second sensitivity experiment with a large upper-level wind speed (Case 4) shows the importance of the synoptic-scale wind speed (Fig. 12d). Clearly, the maximum value of the surface wind speed in Case 4 is comparable to that in Case 2, which is larger than that in Case 1. In addition, the diurnal variation of the wind speed in Case 4 is similar to that in Case 2. The maximum value of the diffusion coefficient in Case 4 is comparable to that in Case 1 (Fig. 13a). However,

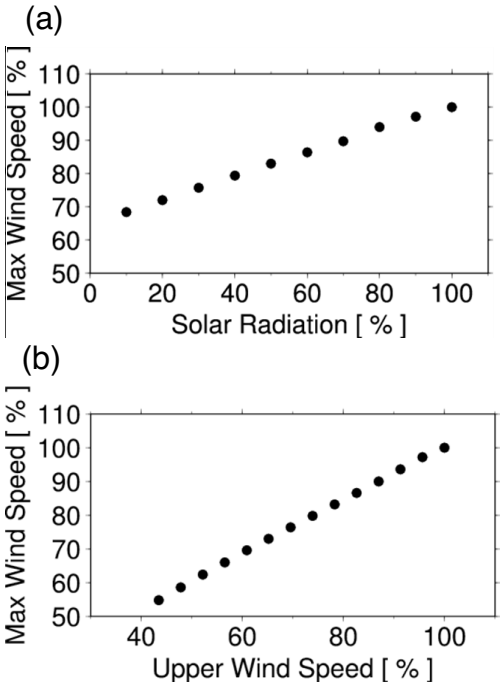

Fig. 14. Results from the additional numerical experiments. Sensitivity of the surface wind speed to (a) solar radiation and (b) upper-level wind speed. It is noted that the weak wind days has 90% solar radiation of the strong wind days on average and 63% upper-level wind speed on average of the strong wind days.

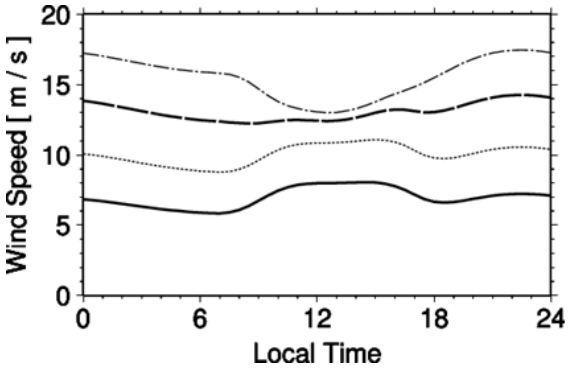

Fig. 15. Same as Figure 12, but for Case 5.

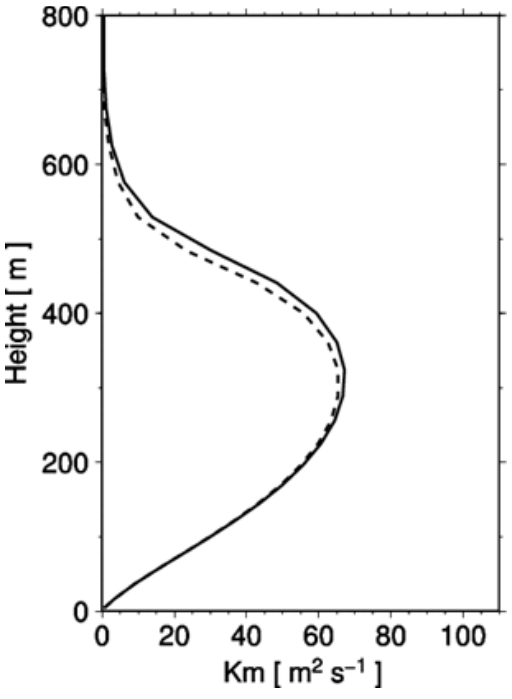

Fig. 16. Same as Figure 13a, but for Cases 2 and 5. Solid and broken lines indicates Cases 2 and 5.

the momentum transfer in Case 4 is much larger than that in Case 1 (Fig. 13b) due to larger wind shear. In addition, the PBL height is larger in Case 4 than in Case 1 (Figs. 13a, b).

A third sensitivity experiment with a stable atmospheric condition (Case 5) shows that the small difference in the background atmospheric stability between the strong and weak-wind days has almost no impact on the surface wind speed (Fig. A1).

Figure 14 contains the results from the additional numerical experiments, which indicate that both the amount of solar radiation and the speed of the upper-level wind have a positive correlation with the daily maximum surface wind speed. However, the impact of the amount of enhanced solar radiation is relatively small considering that weak-wind days receive 90% solar radiation amount, on average, relative to strong wind days. On the other hand, the upper-level wind has a more significant impact than the amount of solar radiation because weak-wind days have 63% upper-level wind speed, on average, relative to strong wind days.

5. Discussion

The results from the numerical simulation in Chapter 4 show that the PBL height at 1400 JST is approximately 700 m on strong-wind days, 650 m on medium-wind days, and 550 m on weak-wind days. On the other hand, at 1400 JST, at which time the surface wind speed

is maximized, the wind speed at the PBL height (measured with a wind profiler, Fig. 7) is 12.8 m s^{-1} on strong-wind days, 8.8 m s^{-1} on medium-wind days, and 4.6 m s^{-1} on weak-wind days. Normalizing the surface wind speed (7.2 m s^{-1} on strong-wind days, 5.3 m s^{-1} on medium-wind days, and 3.2 m s^{-1} on weak-wind days), the surface wind speed is 0.59 on strong-wind days, 0.59 on medium-wind days, and 0.67 on weak-wind days. The difference in the normalized surface wind days is less than 10% among strong, medium, and weak-wind days, although the wind speed on weak-wind days is slightly greater. This suggests that the surface wind speed is closely related to the upper-level wind speed.

However, the present study does not focus on the terrain effects. Mountains enhance the summertime low-level jet over the Kanto Plain and produce a diurnal variation (Kimura and Arakawa 1983), thus the underestimation of the wind speed in the present study could be due to the lack of consideration of the mountainous terrain. Considering the shape of the Kanto Plain and its surrounding mountains, the Karakkaze could have the characteristics of gap winds and flow over the mountains (Fujibe et al. 1999, Rikiishi and Yomogida 2006). Unfortunately, there is no conventional observational data to support or reject this idea. The present simulations also assume a constant geostrophic wind velocity in the vertical direction, which implies no thermal wind and produces some model errors. Numerical experiments using a more realistic three-dimensional model, such as the WRF model (e.g., Skamarock et al. 2008, Kusaka 2009), NHM (e.g., Saito et al. 2007), and CReSS (e.g., Tsuboki and Sakakibara 2001) are expected in future studies.

6. Conclusions

In the present study, the vertical structure of the Karakkaze is climatologically investigated. Furthermore, the impacts of the amount of solar radiation and synoptic-scale wind on the Karakkaze are statistically and numerically examined. The results are summarized as follows.

1. It is statistically confirmed that the Karakkaze often appears in the fan-shaped area surrounded by the Arakawa River, Tonegawa River, and Tokyo Bay. Strong wind areas expand southeastward as the surface wind in Maebashi becomes stronger.

2. On strong-wind days, the surface wind speed has a clear diurnal variation with a peak in the early afternoon as described in the previous study. The daytime wind speed is strong, but the wind weakens at night. Such a diurnal variation pattern is observed up to 200 m, but the pattern nearly reverses itself from the 200 m to 400 m level. On weak-wind days, the diurnal variation pattern reverses itself at 100 m, which indicates that the wind shear is smaller in the lower boundary layer in the daytime and the surface affects the wind at the lower level.

3. Regarding the development of the surface inversion layer that is related to the nocturnal weak wind, strong-wind days are the smallest and the weak-wind days are the largest of the three categories.

4. Statistical analysis shows that the amount of daily global solar radiation on strong-wind days is 0.5 MJ m^{-2} and 1.0 MJ m^{-2} larger than that of medium and weak-wind days, respectively. The correlation coefficient is 0.284 between the daily maximum surface wind speed and daily sunshine duration, which is suggested in a previous study to be the most significant factor.

5. The background potential temperature lapse rate between 925 hPa and 500 hPa on strong-wind days is less stable than that on weak-wind days, but the difference is very small.

6. The surface wind is strengthened when the winter-type pressure pattern is more obviously seen, the east-west pressure gradient over the Japan Islands is larger, and the center of low pressure is located closer to the Japan Islands. Statistical analysis of wind profiler data shows that the wind blows more strongly when the upper-level wind is stronger and the wind shear in the lower boundary layer is larger. The correlation coefficient is 0.632 (confidence interval 99%).

7. Numerical experiments using a simple column PBL model show that a large amount of solar radiation would be a necessary condition for the appearance of the strong daytime wind but is not sufficient to explain the difference in the surface wind speed between weak and strong-wind days. Synoptic-scale wind speed, rather than the amount of solar radiation and atmospheric stability, has a larger impact on the formation of a strong surface wind. Such a result is consistent with that from the statistical analysis.

We conclude that the strong Karakkaze is primarily maintained by the downward momentum transfer due to

a sufficient amount of solar radiation and a strong upper-level wind under a clear winter-type synoptic condition.

Acknowledgements

The tower data was provided by the Meteorological Research Institute, Japan Meteorological Agency (JMA/MRI). We thank Dr. Shigeru Onogi and Dr. Ahoro Adachi of the MRI for their technical comments on the quality of the tower data. We also thank the Editor (Dr. Ichiro Tamagawa of Gifu University) and Dr. Fujio Kimura of the JAMSTEC for their helpful comments in reply to the reviewers. Several comments and points of encouragement from Dr. Masatoshi Yoshino (a professor emeritus at the University of Tsukuba) and Dr. Fumiaki Fujibe of the JMA/MRI helped to summarize the article. Special thanks go to Dr. Masahito Ishihara of the JMA/MRI for his comments on the accuracy of the wind profiler data. This study was supported by the Environment Research and Technology Development Fund (S-8-1(2)) of the Ministry of the Environment, Japan. This study was partly supported by a Grant-in-Aid for Scientific Research from JSP (Grant-in-Aid for Young Scientists (B) 20700667). The Generic Mapping Tools (GMT) was used for the figures.

References

Arakawa, S., 1971: On the local strong winds. *Tenki*, **18**, 103–115 (in Japanese).

Arya, S. P., 2001: *Introduction to micrometeorology*. 2nd Ed. Academic press, 420 pp.

Blackadar, A. K., 1957: Boundary layer wind maxima and their significance for the growth of nocturnal inversion. *Bull. Amer. Meteor. Soc.*, **38**, 283–290.

Furukawa, T., 1966: On the "Yamaji wind". *Tenki*, **8**, 261–268 (in Japanese).

Fujitani, T., 1985: Characteristics of the diurnal variation and spectrum of wind speed in the atmospheric boundary layer at the Tsukuba Science City. *Tenki*, **32**, 259–269 (in Japanese).

Fudeyasu, H., T. Kuwagata, Y. Ohashi, S. Suzuki, Y. Kiyohara, and Y. Hozumi, 2008: Numerical study of the local downslope wind "Hirodo-Kaze" in Japan. *Mon. Wea. Rev.*, **136**, 27–40.

Fujibe, F., K. Saito, D. S. Watt, and S. G. Bradley, 1999: A numerical study on the diurnal variation of low-level wind in the lee of a two-dimensional mountain. *J. Meteor. Soc. Japan*, **77**, 827–843.

Garratt, J. R., 1992: *The atmospheric boundary layer*. Cambridge university press. 316 pp.

Ishii, S., K. Sasaki, K. Mizutani, T. Aoki, T. Itabe, H. Kanno, D. Matsushima, W. Sha, A. Noda, M. Sawada, M. Ujiie, Y. Matsuura, and T. Iwasaki, 2007: Temporal evolution and spatial structure of the local easterly wind "Kiyokawa-Dashi" in Japan PART I: Coherent Doppler Lidar Observations". *J. Meteor. Soc. Japan*, **85**, 797–813.

Kawamura, T., 1966: Surface wind systems over central Japan in the winter season: with special reference to winter monsoon. *Geograph. Rev. Japan*, **39**, 538–554 (in Japanese).

Kimura, F., and S. Arakawa, 1983: A numerical experiment on the nocturnal low level jet over the Kanto plain. *J. Meteor. Soc. Japan*, **61**, 848–861.

Kondo, J. (ed.), 1994: *The meteorology in a water environment*. Asakura-shoten, 350 pp. (in Japanese).

Kusaka, H., 2009: About a regional atmospheric model, WRF. *Nagare*, **28**, 3–12. (in Japanese)

Kusaka, H., and F. Kimura, 2004a: Coupling a single-layer urban canopy model with a simple atmospheric model: Impact on urban heat island simulation for an idealized case. *J. Meteor. Soc. Japan*, **82**, 67–80.

Kusaka, H., and F. Kimura, 2004b: Thermal effects of urban canyon structure on the nocturnal heat island: Numerical experiment using a mesoscale model coupled with an urban canopy model. *J. Appl. Meteor.*, **43**, 1899–1910.

Kusaka, H., F. Kimura, H. Hirakuchi, and M. Mizutori, 2000: The effects of land-use alteration on the sea breeze and daytime heat island in the Tokyo metropolitan area. *J. Meteor. Soc. Japan*, **78**, 405–420.

Louis, J. F., 1979: A parametric model of vertical eddy fluxes in the atmosphere. *Bound.-Layer Meteor.*, **17**, 187–202.

Mellor, G. L., and T. Yamada, 1974: A hierarchy of turbulence closure models of planetary boundary layers. *J. Atmos. Sci.*, **31**, 1791–1806.

Miya, Y., and H. Kusaka, 2009: Climatological study on the diurnal variation and spatial distribution of the Karakkaze wind on the Kanto Plain. *Geograph. Rev. Japan*, **82**, 346–355. (in Japanese)

Nakamura, M., M. Joko, O. Tsukamoto, T. Kanamori, K. Azuma, K. Kawata, H. Kimura, N. Kamei, T. Kamata, and H. Fudeyasu, 2002: Experimental study of the downslope wind ("Hiroto-Kaze") occurrence at Mt. Nagi. *Tenki*, **49**, 129–139 (in Japanese).

Rikiishi, K., and Y. Yomogita, 2006: On the generation of the strong northwesterly winds in the Tokachi plain. *Tenki*, **53**, 773–784 (in Japanese).

Saito, K., and M. Ikawa, 1991: A numerical study of the local downslope wind "Yamaji-kaze" in Japan. *J. Meteor. Soc. Japan*, **69**, 31–56.

Saito, K., 1994: A numerical study of the local downslope wind "Yamaji-kaze" in Japan. Part 3: Numerical simulation of the 27 September 1991 windstorm with a nonhydrostatic multi-nested model. *J. Meteor. Soc. Japan*, **72**, 301–329.

Saito, K., J. Ishida, K. Aranami, T. Hara, T. Segawa, M. Narita, and Y. Honda, 2007: Nonhydrostatic atmo-

spheric models and operational development a JMA. *J. Meteor. Soc. Japan*, **85B**, 271–304.

Sasaki, K., M. Sawada, S. Ishiim, H. Kanno, K. Mizutani, T. Aoki, T. Itabe, D. Matsushima, W. Sha, A. T. Noda, M. Ujiie, Y. Matsuura, and T. Iwasaki, 2010: The temporal evolution and spatial structure of the local easterly wind "Kiyokawa-dashi" in Japan. Part II: Numerical simulations. *J. Meteor. Soc. Japan*., **88**, 161–181.

Skamarock, W. C., J. B. Klemp, J. Dudhia, D. O. Gill, D. M. Barker, M. G. Duda, X.-Y. Huang, W. Wang, and J. G. Powers, 2008: A description of the advanced research WRF version 3. NCAR/TN-475+STR, 113pp.

Takeuchi, M., 1986: On the local strong winds in the middle part of Shonai Plain of Yamagata prefecture. *Tenki*, **33**, 219–231 (in Japanese).

Tsuboki, K., and A. Sakakibara, 2001: CReSS User's Guide. 2nd Ed., 210pp. (in Japanese).

Yomogida, Y., and K. Rikiishi, 2004: *Diurnal variation of the strong local wind "Karak-Kaze" in the Kanto Plain with special reference to the role of thermal convection*. Proc. 18th Wind Eng. Sympo, 23–28 (in Japanese).

Yamagishi, Y., 2002: *Essentials of wind for weather forcasting.* Ohmsha, 189 pp. (in Japanese).

Yamagishi, Y., and H. Katoh, 1996: Statistical properties and environmental synoptic features of strong wind around Miyagi prefecture. *Journal of Meteorological Research*, **48**, 15–32 (in Japanese).

Yamamoto, G., A. Shimanuki, M. Aida, and N. Yasuda, 1973: Diurnal variation of wind and temperature fields in the Ekman layer. *J. Meteor. Soc. Japan*, **51**, 377–387.

Yoshino, M. M., 1970: Oroshi; ein starker Lokalwind in der Kanto Ebene, Japan, *Colloquium Geographicum*, **12**, 43–57.

Yoshino, M. M., 1986: *Climate in a small area. New Ed.* Chijin Shokan, 298 pp. (in Japanese).